Journal of Theoretical and Applied Physics (JTAP), Special Issue: AICIS'23-Article 19

Proceeding of the 3rd Annual International Conference on Information and Sciences 2023, University of Fallujah, Iraq

https://dx.doi.org/10.57647/j.jtap.2024.si-AICIS23.19

Comparison between plasma distribution in plane and concave cathodes DC discharge systems

Mohammed O. Salman[1,*], Wasan Abd Al-Rahman Khalaf[2], Barakat O. Ahmed[3]

[1]*Department of Medical Physics, College of Applied Science, University of Fallujah, Iraq.*
[2]*Ministry of Education, Iraq.*
[3]*Ministry of Education, Anbar Educational Directorate, Anbar, Iraq.*

[*]**Corresponding author:** dr.mohammedodehsalman@uofallujah.edu.iq

Original Research

Published online: 15 June 2024

Abstract:

Computer simulation has become an integral component of scientific and engineering activities, particularly in the realm of design optimization. This study employs the finite element method (FEM) through COMSOL-Multiphysics software (Version 4.0) to simulate direct current discharge plasma within argon gas under vacuum (2×10^{-1} mbar). The primary objective is to compare the plasma distribution characteristics resulting from two distinct cathode configurations: a planar cathode, and a concave cathode. The findings of this investigation demonstrate a noteworthy disparity in the distribution of plasma between the two cathode designs. The substitution of the planar cathode with the concave variant leads to a considerable confinement of the plasma within a more delimited spatial region, specifically at a particular point within the system. Moreover, notable variations are observed in the spatial distribution of critical parameters such as electron temperature, electron density, and positive ions density. Furthermore, the spatial distribution of the space charge is markedly dissimilar in the configuration featuring the concave cathode. It is inferred that the plasma zone experiences a unique spatial arrangement in this scenario, with the plasma being confined predominantly in close proximity to the z-axis, but encompassing a larger circular region at 1.5 cm away from the cathode.

Keywords: Simulation; DC discharge; Plasma distribution

1. Introduction

Computer simulation is defined as a translation of the real world into its virtual form using basic physics laws to predict the practical results within several variables in the design and process parameters to reach the optimal model design and conditions before starting to implement the design [1]. Nowadays, computer simulation has become an important part of science and can employed in many fields [2].

Plasma discharge under low pressure can be described by two common computational models: Particle-In-Cell (PIC) model and the fluid model [3]. In the PIC method, plasma is represented by discrete computational units, each of which models a large number of real particles with both charge and mass [3]. This discretization optimizes simulations for computational efficiency while maintaining accuracy [4]. In the fluid model, plasma species are treated as a fluid, and their kinetics are described using fluid equations [5]. Various types of collisions between species are treated as isolated problems [6]. The fluid model was based on the density continuity and mean energy of the basic species; the flux equations within the plasma and Poisson's equation were coupled to find an approximate solution [7]. The flux equations include a diffusion term caused by density gradients and a drift term for the charged particles affected with force by an electric field [8, 9].

COMSOL Multiphysics is based on the finite element method used in many scientific fields [10]. The differential equations were solved numerically at a finite number of points within the region of interest [11, 12]. There are two main ways to present the huge amount of digital output data from plasma simulation: by calculating the mean values, which can be compared directly with the experimental values, or by visualization of the plasma, which gives a spatial

presentation of the phenomena within the plasma by using the color gradient to represent the change of quantities and measurements such as plasma species densities or reactions rates etc. [13].

2. Mathematical model

Finite element modeling (FEM) was used to make simulation by solving, numerically, differential equations based on drift-diffusion approximation, in dc gas discharge, for electron density (n_e), ion density (n_i), and mean electron energy (n_ε) conservation equations, coupled with Maxwell equations.

The model includes continuity equations for the four dominant species, the electrons, positive ions, neutral atoms, and metastable atoms [14].

$$\frac{\partial n_j}{\partial t} + \nabla.\Gamma_j = S_j \tag{1}$$

where S_j is the particle formation rate in plasma reactions and Γ_j is the particle flux, which is defined according to drift-diffusion approximation as [15]:

$$\Gamma_j = \pm n_j \mu_j E - D_j \nabla n_j \tag{2}$$

where μ and D represent the mobility and diffusion coefficients. The first term takes a positive sign for ions, a negative sign for electrons, and vanished for non-charged species. The gradient in electric field (E) is estimated by Poisson's equation [16]

$$\varepsilon_0 \nabla.E = \Sigma_j q_j n_j \tag{3}$$

where ($E = -\nabla\emptyset$)

While the mean electron energy (n_ε) conservation equations [17]

$$\frac{\partial N_\varepsilon}{\partial t} + \nabla.[-n_\varepsilon(\mu_\varepsilon.E) - D_\varepsilon.\nabla\varepsilon] + E.\Gamma_e = S_\varepsilon \tag{4}$$

The electron energy mobility and diffusion coefficients (μ_ε and D_ε) defined as [18]:

$$\mu_\varepsilon = \frac{5}{3}\mu e D_\varepsilon = \mu_\varepsilon T_e \tag{5}$$

Free electrons will be accelerated by electric field to thermal velocity ($\bar{\upsilon}$) which derived using Maxwell-Boltzmann distribution is [19]

$$\bar{\upsilon} = \left(\frac{8k_B T_e}{\pi m_e}\right)^{\frac{1}{2}} \tag{6}$$

where k_B represents Boltzmann constant And along its way, they collide with the gas atoms in four collision types, elastic, excitation, ionization reaction and step-wise ionization. These collisions obey the collision cross-section for this type, which depends on electron energy [20]. The electron-atom collision cross sections for argon were taken from [21].

2.1 Simulation preparation

Two dimensional (axial-symmetric model) for low-pressure argon dc discharge using COMSOL Multiphysics software, with drift-diffusion approximation, were chosen to design the two configurations (plane and concave cathodes).

Cylindrical chamber with 5 cm radius and 8 cm height was assumed, dc-power supply varied linearly with time from 300 to 500 volt.

Figure 1 illustrates the right side of a longitudinal cross-section for the two electrode configurations (with the plane and concave cathodes) using the 2D axisymmetric model and their mesh distributions. Disc cathode with 2 cm radius and hemispherical cathode with 2 cm radius were used; disc anode with 2 cm radius and the electrodes separation is 2 cm were used. Fine mesh elements are required at a high potential gradient near the electrodes, while large mesh elements were used at the points has a small electric field to reduce solution time. Gradually, variation in size was controlled between adjacent mesh elements.

Four types of species were assumed at the discharge region, which are the dominant species in argon discharge, as shown in Table 1.

The dominant gas phase and surfaces reactions which used in simulation and their related energy difference were shown in Table 2.

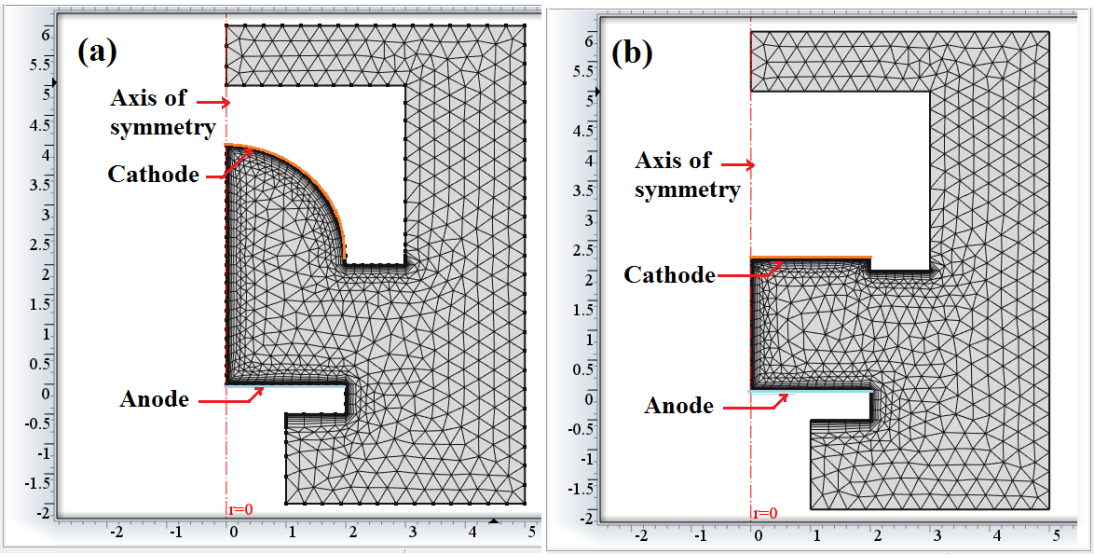

Figure 1. Two-dimensional geometry and used mish distribution in simulation for (a) concave and (b) plane cathode design.

Table 1. The species used in the simulation. (e and m_e) represent the electron charge and mass, respectively.

Species	Symbol	Charge	Mass
Electron	e	$-e$	m_e
Neutral argon atom	Ar	0	39.94 amu
Argon ion	Ar+	e	39.94 amu
Excited argon atom	Ar*	0	39.94 amu

E_{ion} (Ar) represents the first ionization energy for Ar = 15.759 eV [17], φ_{Cu} is the work functions of cathode metal (which is assumed as copper) φ_{Cu} = 4.51 eV [22].
The calculation is based on the drift-diffusion approximation equation model using the "built-in Plasma Module", subject to the boundaries shown in Fig. 1.
The simulation software operates according to initial data, wherein gas atoms are uniformly dispersed to achieve consistent density for each element in accordance with the assumed pressure of 2×10^{-1} mbar and an initial zero potential. The prevailing conditions are determined by computing the requisite quantities across all finite elements within a closed calculation cycle. Subsequently, the simulation estimates the necessary step time for calculations based on the percentage of errors that manifest during the computational process. At each step, the software calculates the potential, then the electric field in each element the change in the flow for each species, and the change in their densities using the continuity equation; these variations are then added to the stored values from the previous step. The program finishes when the assigned time is over.

3. Results and discussions

This section presents simulation results for basic plasma properties, including excitation reaction rate, electron density, plasma temperature, charged species densities and space charge density for the two cathode configurations (plane and concave cathodes).
The regions of plasma emission can be estimated by studying the regions with considerable excitation reactions. As shown in Fig. 2, a small excitation rate appeared, so no light emission can occur. Large potential causes anode potential screening and extended towards the cathode which causes increasing and shifting the maximum of excitation rate towards the cathode. The results of the simulation compare the performance of concave and plane cathodes in a DC discharge plasma system, specifically at an applied voltage of 500 volts and the constant pressure of 0.2 mbar. This comparison primarily focuses on the excitation rate distribution within the plasma. Regardless of whether the cathode is concave or plane in shape, the electric field is oriented vertically on the cathode surface. This means that both cathode shapes have an equipotential surface, ensuring that the electric field strength is consistent for the simulation. Electrons require a certain distance from the cathode surface to obtain sufficient energy for exciting atoms within the plasma. This observation highlights the importance of electron energy distribution and the role of the cathode in facilitating this process. Within a specific range of electron energies, the cross-section for excitation collisions is larger. This range likely corresponds to the energy levels at which electrons are most effective at exciting atoms in the plasma. An interesting finding is that the shape of the glow region within the plasma approximately mirrors the shape of the electrode surface. In the case of the concave cathode, this implies that the glow appears within the cavity. This observation suggests that the geometry of the cathode has a significant impact on the distribution and localization of the plasma glow. These results show the differences between concave and plane cathodes in a DC discharge plasma system, particularly regarding excitation rates and the shape of the resulting glow region.
The additional insights provided in Fig. 3 regarding electron number density distribution in the two cathode shapes at different applied voltages (300 volts and 500 volts) enhance

Table 2. Plasma interactions in simulation.

Reaction	Description	Location	Losses energy (eV)
e+ Ar => e+ Ar	Elastic collision	gas	0
e+ Ar => e+ Ar*	Excitation collision	gas	11.5
e+ Ar => 2e+ Ar+	Ionization collision	gas	15.759
e+ Ar* => 2e+ Ar+	Stepwise ionization	gas	4.42
Ar+ => Ar	Recombination	Non cathode walls	-
Ar* => Ar	De-excitation reaction	All walls	-

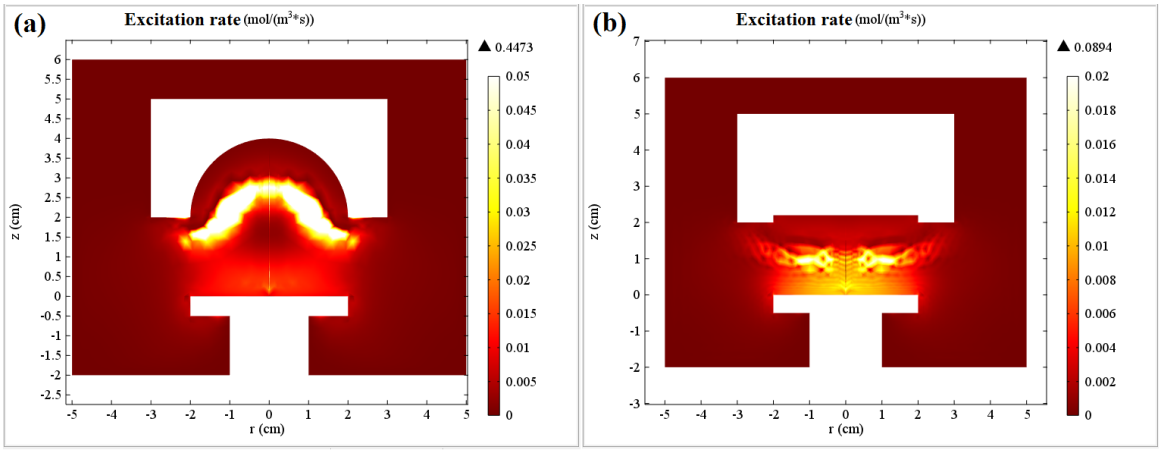

Figure 2. Excitation reaction rate distributions for (a) concave and (b) plane cathode design.

our understanding of the comparison between concave and plane cathodes in the DC discharge plasma system. The applied voltage plays a crucial parameter in shaping electron number density distribution. At the lower voltage of 300 volts, a noticeable region of higher electron density forms in front of the anode. This observation implies that ionization processes are less frequent at lower voltages, predominantly occurring near the anode. As the applied voltage is increased to 500 volts, the high-density region moves across the discharge gap. This shift signifies an augmented ionization rate in response to the stronger electric field. Consequently, electrons attain the necessary ionization energy more readily, leading to a more evenly spread electron number density throughout the discharge gap.

The ionization rate is intimately connected to the presence of ionized particles in the plasma, which, in turn, affects the electron population. Higher electric field strengths shorten the distance needed for electrons to acquire sufficient ioniza-

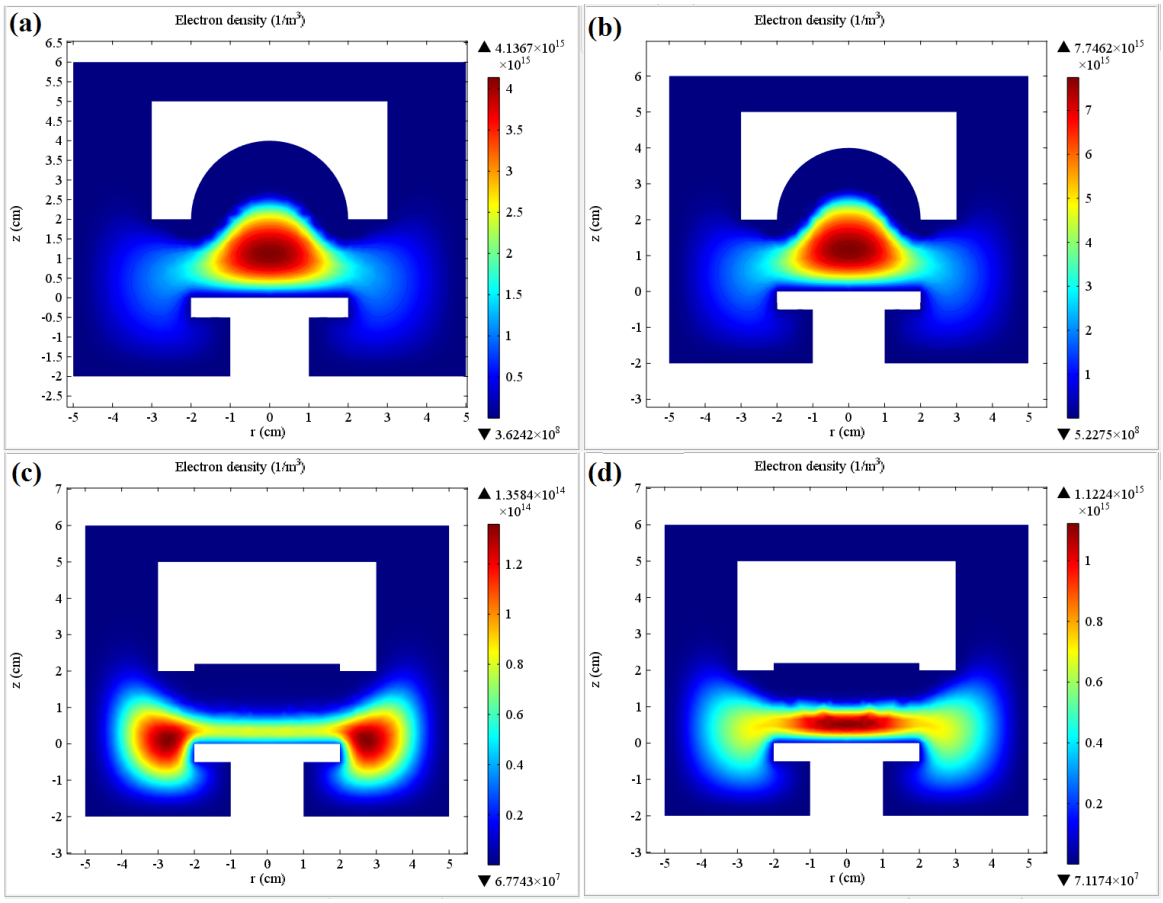

Figure 3. Electron number density distributions at different applied voltage and different cathode design (a) concave (300 V) (b) concave (500 V) (c) plane (300 V) and (d) plane (500 V).

tion energy. This is a consequence of the more rapid electron acceleration within the stronger electric field. Conversely, at lower voltages (e.g., 300 volts), ionization predominantly occurs near the anode, necessitating a longer electron travel distance to achieve the energy required for ionizing neutral atoms. At lower voltages, where the voltage gradient is nearly uniform between the electrodes, electrons initiating ionization near the anode trigger electron avalanches, leading to an accumulation of electrons. This accounts for the observed peak in electron density near the anode at the beginning of the discharge under low voltage conditions. Increasing electron density, primarily through secondary electron emission and electron avalanches in the discharge gap, results in a high potential gradient near the cathode. This scenario is due to the voltage difference being concentrated within the cathode sheath, shifting the maxima of electron number density toward the cathode.

Fig. 4 illustrates the electric field lines and direction with plasma density distribution at 500 V applied voltage for the two cathode designs. It seems that the electric field profile is directed from the plasma towards the walls. Since the electric fields are directed from the plasma towards the walls due to positive sheath potential, the electrons are confined and concentrates at the point where the electric field inverses. It can be seen that the zero electric fields focused on a specific point with a concave cathode while appearing as the plane region with the plane cathode. This is why we observe the concentration of the plasma density in a limited space while the density is spread over a wider area in the flat-cathode model.

Studying the electron temperature distribution is very important to the special probability of different plasma reactions. Fig. 5 shows the electron temperature distribution for the two designs at 300 and 500 volt applied voltage. The large voltage drop in the cathode fall caused an increase in the electron temperature rapidly at this region. The higher electron temperature appeared at the region with the same distance from the cathode walls, so this region has approximately the same as the cathode shape.

In order to understand the breakdown process more fully in the two designs, one-dimensional curves of plasma density, plasma temperature, positive ion density and space charge density behaviors were investigated on the line of symmetry.

Fig. 6 illustrates the increment of electron density distribution for the two designs with increasing the applied voltage along the axis of symmetry, and in the concave cathode, the density maximum is greater than that in the plane design. It is obvious that the electron density maximum exists within the plasma region, which spreads within a specific region, in concave cathode design larger than that in-plane cathode design, which appeared limited at a narrow distance. The electron in the negative glow appeared with a very small density.

The electron temperature distribution shows a maximum in the cathode sheath. Increasing the applied potential causes an increase in the plasma temperature maximum and narrows toward the cathode due to reducing plasma sheath with increasing plasma density. The comparison between the two designs illustrates that the electron temperature distribution is limited in the narrow region inside the hollow cathode. At the same time, the peak spread at the larger region in the plane cathode design as shown in Fig. 7.

Fig. 8 shows the simulation result for argon ion density distributions at the axis of symmetry between the two electrodes from disc and concave cathodes using different applied voltages from 300 to 450 volt. The positive ion density is slightly higher than the electron density in the negative glow, while reversing at the cathode sheath region. The space charge density distribution study is the most important way to recognize the different regions of the glowdischarge. Positively charged sheath regions are formed near the two electrodes in contact with the plasma. The development of different space charge regions is due to the mass difference between electrons and ions, i.e. their mobility. The high electron speed near the electrode leadd to the formation of net positive space-charge regions. Electrons are confined within the plasma while the positive ions enter the sheath

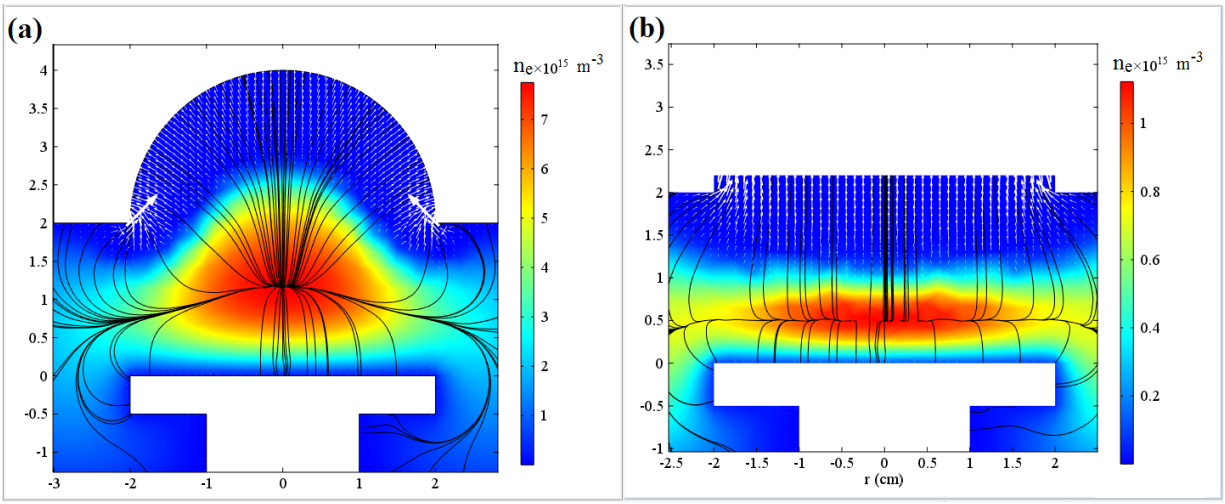

Figure 4. Electric field lines and plasma density at 500 V applied voltage for the two cathode designs (a) concave and (b) plane cathode.

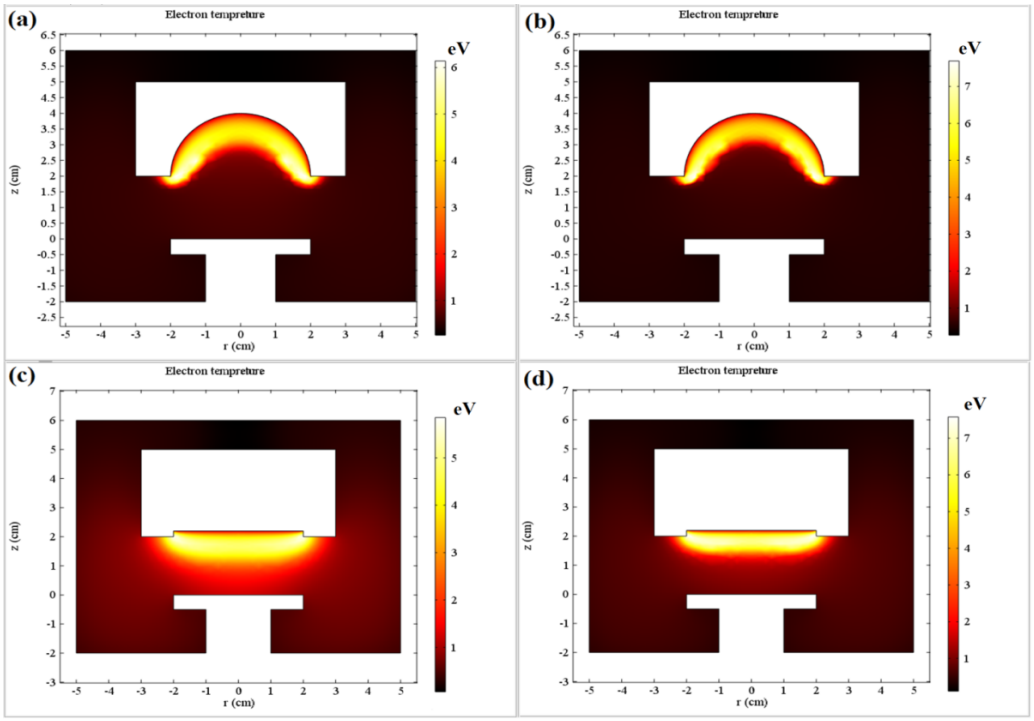

Figure 5. Plasma temperature distributions at different applied voltage and different cathode designs: (a) concave/300 V, (b) concave/500 V, (c) plane/300 V, and (d) plane/500 V.

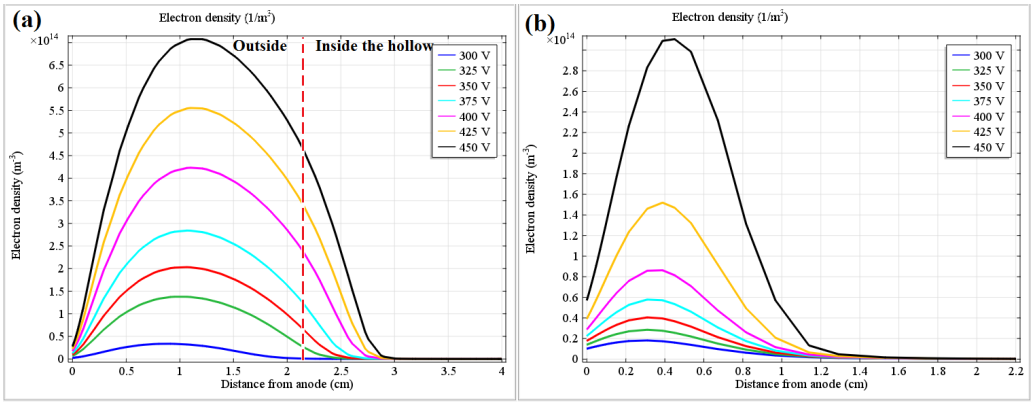

Figure 6. Plasma density distributions at line of symmetry using different applied voltage for (a) concave and (b) plane cathode design.

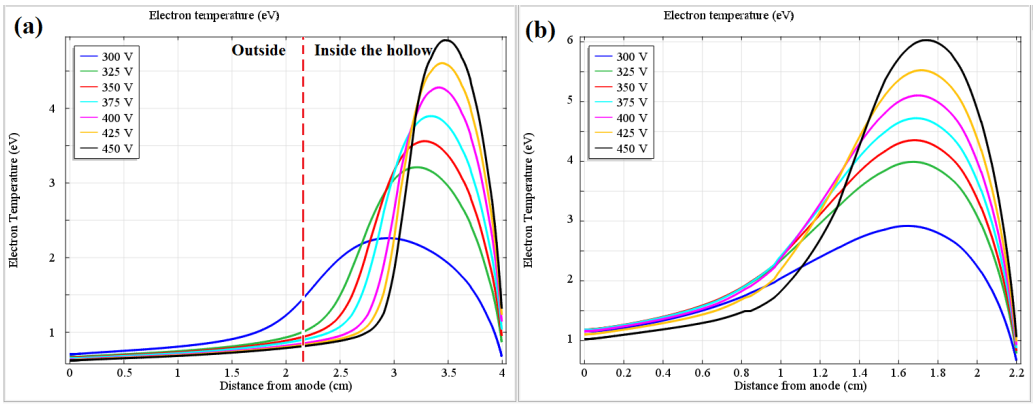

Figure 7. Electron temperature distributions at the axis of symmetry using different applied voltages for (a) concave and (b) plane cathode configurations.

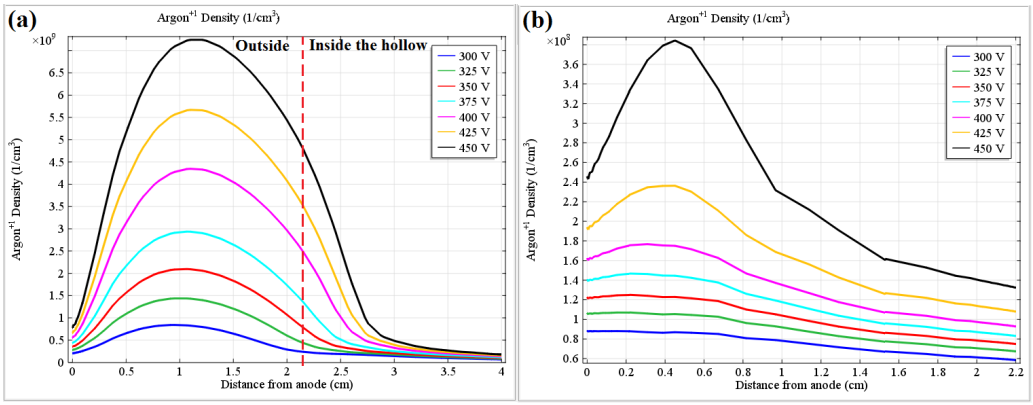

Figure 8. Argon ion density distributions at the line of symmetry using different applied voltage for (a) concave and (b) plane cathode design.

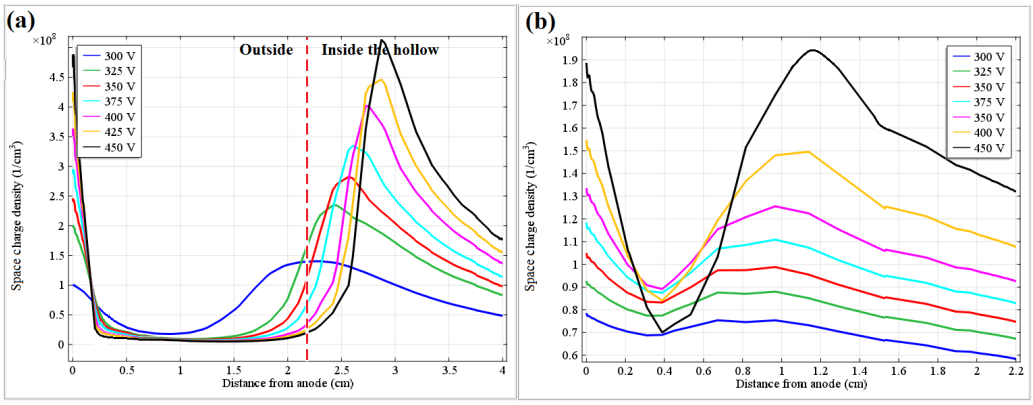

Figure 9. Space charge density distributions at the line of symmetry using different applied voltage for (a) concave and (b) plane cathode design.

region and attracted toward the cathode [23].
In the plane cathode model, the plasma region (the quasi neutral regions) appears as narrow zone at about 0.4 cm from anode in the z-axis direction. In hollow cathode configuration this region extended to wider zone from 0.2 to 2 cm from the anode and increases to 2.5 cm with increasing applied voltages as shown in Fig. 9.

4. Conclusion

In this work, simulation for dc discharge in argon gas for two cathode types (plane and concave cathode) using a 2D axial symmetric model by COMSOL software (Version 4.0). The study showed that plasma could be confined within a narrow space using an electric field by changing the cathode configuration without using a magnetron. Where the study showed that the concave cathode with hemisphere configuration limits the plasma within a narrow zone better than the flat cathode. This configuration of the concave cathode works well to converge the electron beam and reduce particle loss to the chamber wall for use in electron guns.

Authors Contributions
Authors have contributed equally in preparing and writing the manuscript.

Availability of data and materials
Data presented in the manuscript are available via request.

Conflict of Interests
The author declare that they have no known competing financial interests or personal relationships that could have appeared to influence the work reported in this paper.

References

[1] A. L. Kritcher, C. V. Young, and H. F. Robey. "Design of inertial fusion implosions reaching the burning plasma regime.". *Nat. Phys.*, **18**:251–258, 2022. DOI: https://doi.org/10.1038/s41567-021-01485-9.

[2] C. Jia, J. Linhong, W. Kesheng, H. Chuankun, and S. Yixiang. "Two-dimensional simulation of inductively coupled plasma based on COMSOL and comparison with experimental data.". *J. Semicond.*, **34**:1–7, 2013. DOI: https://doi.org/10.1088/1674-4926/34/6/066004.

[3] M. Y. Hur, J. S. Kim, I. C. Song, J. P. Verboncoeur, and H. J. Lee. "Model description of a two-dimensional electrostatic particle-in-cell simulation parallelized with a graphics processing unit for plasma discharges.". *Plasma Res. Express.*, **1**, 2019. DOI: https://doi.org/10.1088/2516-1067/ab0918.

[4] J. Candy, I. Sfiligoi, E. Belli, K. Hallatschek, C. Holland, N. Howard, and E. D'Azevedo. "Multiscale-optimized plasma turbulence simulation on petascale architectures.". *Comput. Fluids.*, **188**:125–135, 2019. DOI: https://doi.org/10.1016/j.compfluid.2019.04.016.

[5] M. Abdollahzadeh, J. C. Pascoa, and P. J. Oliveira. "Implementation of the classical plasma–fluid model for simulation of dielectric barrier discharge (DBD) actuators in OpenFOAM.". *Comput. Fluids.*, **128**:77–90, 2016. DOI: https://doi.org/10.1016/j.compfluid.2016.01.012.

[6] Á. Sánchez-Villar, J. Zhou, E. Ahedo, and M. Merino. "Coupled plasma transport and electromagnetic wave simulation of an ECR thruster.". *Plasma Sources Sci. Technol.*, **30**:045005, 2021. DOI: https://doi.org/10.1088/1361-6595/abde20.

[7] K.-L. Chen, M.-F. Tseng, M.-C. Lo, S. Hamaguchi, M.-H. Hu, Y.-M. Lee, and J.-S. Wu. "Development of a massively parallelized fluid-based plasma simulation code with a finite-volume method on an unstructured grid.". *IEEE Trans. Plasma Sci.*, **49**:104–119, 2021. DOI: https://doi.org/10.1109/TPS.2020.3013632.

[8] H. Wang and J. Du. "The diffusion and anomalous diffusion of charged particles in the plateau regime of toroidal plasma. ". *Chinese J. Phys.*, **75**:169–186, 2022. DOI: https://doi.org/10.1016/j.cjph.2021.11.028.

[9] H. C. Kim, F. Iza, S. S. Yang, M. Radmilović-Radjenović, and J. K. Lee. "Particle and fluid simulations of low-temperature plasma discharges: benchmarks and kinetic effects. ". *J. Phys. D. Appl. Phys.*, **38**:R283–R301, 2005. DOI: https://doi.org/10.1088/0022-3727/38/19/R01.

[10] R. K. Saini, A. Kumar, V. Goyal, A. Agarwal, and R. Prajesh. "Evaluating EM-field enhancement of different shapes of metallic nanoparticles using COMSOL multiphysics for SERS-based sensors.". *Mater. Today Proc.*, **76**:383–387, 2023. DOI: https://doi.org/10.1016/j.matpr.2022.11.425.

[11] E. Bourne, P. Leleux, K. Kormann, C. Krusea, V. Grandgirard, Y. Güçlü, M. J. Kühn, U. Rüde, E. Sonnendrücker, and E. Zoni. "Solver comparison for Poisson-like equations on tokamak geometries. ". *J. Comput. Phys.*, **488**:112249, 2023. DOI: https://doi.org/10.1016/j.jcp.2023.112249.

[12] J. Anagnostopoulos and G. Bergeles. "Corona discharge simulation in wire-duct electrostatic precipitator. ". *J. Electrostat.*, **7**:129–147, 2002. DOI: https://doi.org/10.1016/S0304-3886(01)00172-3.

[13] T. S. Ramazanov, S. K. Kodanova, M. K. Issanova, N. K. Bastykova, and Z. A. Moldabekov. "The modern information technologies and visualizationmethods for analysis of computer simulation results for complex plasma. ". *Commun. Comput. Phys.*, **15**:981–995, 2014. DOI: https://doi.org/10.4208/cicp.140313.070613s.

[14] Q. Wang, D. J. Economou, and V. M. Donnelly. "Simulation of a direct current microplasma discharge in helium at atmospheric pressure.". *J. Appl. Phys.*, **100**: 1–10, 2006. DOI: https://doi.org/10.1063/1.2214591.

[15] I. R. Rafatov, E. A. Bogdanov, and A. A. Kudryavtsev. "Fluid model of DC glow discharge with nonlocal ionization source term. ". *J. Phys. Conf. Ser.*, **406**, 2012. DOI: https://doi.org/10.1088/1742-6596/406/1/012032.

[16] B. M. Smirnov. "Physics of ionized gases.". *John Wiley & Sons*, , 2004. DOI: https://doi.org/10.1109/MEI.2004.1307100.

[17] R. B. Goldston and A. Rutherford. "Introduction to plasma physics.". *Bristol and Philadelphia*, , 1995. DOI: https://doi.org/10.2307/2077150.

[18] O. Lupan, V. Postica, N. Ababii, M. Hoppe, V. Cretu, I. Tiginyanu, V. Sontea, T. Pauporté, B. Viana, and R. Adelung. "Influence of CuO nanostructures morphology on hydrogen gas sensing performances. ". *Microelectron. Eng.*, **164**:63–70, 2016. DOI: https://doi.org/10.1016/j.mee.2016.07.008.

[19] W. M. Stacey. "Fusion plasma physics. ". *WILEY-VCH Verlag GmbH & Co.*, , 2005. DOI: https://doi.org/10.1017/CBO9781107415324.004.

[20] A. Fridman. "Plasma chemistry.". *Cambridge University Press*, , 2008. DOI: https://doi.org/10.1017/CBO9780511546075.

[21] G. Raju. "Electron-atom collision cross sections in argon: an analysis and comments.". *IEEE Trans. Dielectr. Electr. Insul.*, **11**:649–673, 2004. DOI: https://doi.org/10.1109/TDEI.2004.1324355.

[22] M. L. Williams. " Handbook of Chemistry and Physics, 76th Edition. ". *CRC Press*, **53**:504–504, 1996. DOI: https://doi.org/10.1136/oem.53.7.504.

[23] B. M. Penetrante, M. C. Hsiao, B. T. Merritt, G. E. Vogtlin, and P. H. Wallman. "Comparison of electrical discharge techniques for nonthermal plasma processing of NO in N_2.". *IEEE Trans. Plasma Sci.*, **23**:679–687, 1995. DOI: https://doi.org/10.1109/27.467990.